Investigation of the height of the homogeneous aerosol atmosphere in the visible and infrared spectral regions

V.N. Uzhegov, Yu.A. Pkhalagov, D.M. Kabanov, S.M. Sakerin, and M.V. Panchenko

Institute of Atmospheric Optics, Siberian Branch of the Russian Academy of Sciences, Tomsk

Received December 27, 2004

Based on data of simultaneous measurements of the spectral transmittance of the atmosphere in the surface layer and through the entire atmospheric column, the height of the homogeneous aerosol atmosphere was estimated in the wavelength region from 0.44 to 3.9 μm, for the first time, for the summer season of 2002 near Tomsk. The height of the homogeneous aerosol atmosphere was determined as the ratio of the aerosol optical depth $\tau^a(\lambda)$ to the aerosol extinction coefficient $\alpha(\lambda)$. It was found that this height averages about 1100 m in the wavelength range from 0.44 to 0.56 μm, then it gradually decreases down to 690 m near $\lambda = 1.06$ μm. However, further into the IR region, the height H_0 surprisingly begins to grow, and at $\lambda = 3.9$ μm it achieves 1340 m. Assumingly, this can be attributed to the presence of monodisperse particles with the radius of ~ 3 μm in the upper atmospheric layers. The daily dynamics has been revealed in the spectral dependence of the height of the homogeneous aerosol atmosphere. It has been shown that in the morning the dependence $H_0(\lambda)$ has a maximum in the visible, while in the day and evening the maximum moves near $\lambda = 3.9$ μm.

Introduction

In recent years, the problem of climate change on the Earth has been widely discussed in the literature. This problem has arisen from the actually observed increase of the global mean temperature of the air, which is partly caused by the anthropogenic increase of the concentration of CO_2 and other greenhouse gases.[1–3] To evaluate the further development of this process and its social-economic consequences, numerous climatic models have been developed and many accompanying calculations performed using various versions of the possible dynamics of the future accumulation of greenhouse gases (see, for example, Ref. 3). It turned out, however, that the model calculations give widely different estimates due to uncertainties in the important climate-forming parameters, used in the calculations. These parameters include certainly the aerosol of the atmospheric boundary layer (ABL).

The radiative significance of the ABL aerosol is clearly illustrated, in particular, in Ref. 4 with the one-dimensional interactive CAPS (*Coupled Atmosphere–Plant–Soil*) model for the fine weather, taken as an example. It is shown that the aerosol, scattering and absorbing solar radiation in the atmospheric boundary layer, affects the vertical distribution of the radiative heat influx, which causes the changes in the thermal conditions and dynamics of the ABL. In this case, if solar radiation flux is attenuated only due to scattering by aerosol, then the decrease in the sum of the sensible and latent heat leads to moistening of the atmospheric boundary layer and, consequently, to suppression of the evaporation process. However, if the solar radiation flux is attenuated in the presence of an absorbing aerosol, then additional heating of the atmosphere due to this effect can occur, and the boundary layer becomes drier, which favors the evaporation process. The decrease of the sum of the sensible and latent heat leads also to the change of the aerosol buoyancy flux near the surface and thus affects the structure of the ABL inversion.

In the case of a purely scattering aerosol, the decrease of the ABL temperature and the extinction of the buoyancy flux lead to the enforcement of the inversion and to lowering of the upper boundary of the mixing layer. The increase of the ABL temperature (in the case of the absorbing aerosol), on the contrary, can favor the rise of the upper ABL boundary, in spite of the decrease in the buoyancy flux. It was also noted that the presence of the absorbing aerosol in the ABL decreases the probability of cloud formation, which favors the heating of the air.

In general, the calculations[4] have shown that the radiative forcing of the tropospheric aerosol can be different and the accuracy of forecasting the climatic parameters depends significantly on how adequate are the optical and microphysical parameters of the tropospheric aerosol. This determines the urgency of comprehensive field investigations into the optical characteristics of the atmospheric boundary layer.

A promising method of investigation of the ABL optical characteristics is the method based on simultaneous measurements of the aerosol extinction of optical radiation in a wide wavelength region along slant and near-surface paths. In the approximation of the exponential vertical distribution of aerosol, these

0235-6880/05/05–06 367-06 $02.00

investigations can give not only the aerosol optical depth of the atmosphere $\tau^a(\lambda)$ and the aerosol extinction coefficient in the surface layer $\alpha(\lambda)$, but also to estimate the height of the homogeneous aerosol atmosphere in different spectral ranges $H_0(\lambda)$, determined from the equation

$$H_0(\lambda) = \tau^a(\lambda)/\alpha(\lambda).$$

Note that the parameter H_0 is sometimes referred to as the "effective" height of the aerosol atmosphere or the scale height.

Since H_0, by definition, characterizes the height of the mixing layer for particles of different size in different spectral ranges, this parameter can be used to study the dynamics of the mixing layer for both fine and coarse aerosol under different meteorological conditions and states of the underlying surface.

Until recently, there were only few purposeful studies of the height of the homogeneous atmosphere. Here we can note Ref. 5, which revealed the seasonal and daily variability of the parameter H_0 near $\lambda = 0.55$ μm in some regions of Italy. It was shown that the minimum values $H_0(0.55) = 0.5–1.3$ km are observed in fall and winter in the presence of a strong temperature inversion, while the maximum values (2–2.5 km) are observed in summer under urban conditions at a well developed convection. In most cases, H_0 increased in the morning hours with the rate from 30 to 180 m/h due to the increase of the air temperature. Note that in Ref. 5 the values of the coefficient $\alpha(0.55)$ were determined from the observations of the meteorological visual range and were restricted to only fine conditions to provide for the uniform illumination of the observation path.

The spectral measurements of $H_0(\lambda)$ in a wavelength region of 0.37–0.85 μm for five days (late September–early October) were carried out near Odessa.[6] In this case, the values of $\alpha(\lambda)$ were determined instrumentally with spectronephelometers. It was shown that, in this wavelength region, the height of the homogeneous atmosphere decreased from 0.8 to 0.5 km with the wavelength increase.

In Refs. 7 and 8, we considered the values of the parameter $H_0(\lambda)$ measured in the region $\lambda = 0.44–1.06$ μm. The measurements were conducted near Tomsk in the warm seasons of 1995–2000. The spectral coefficients $\alpha(\lambda)$ in the surface layer were determined with an open-path meter of atmospheric transmittance.

It has been found that, on the average, the height of the homogeneous aerosol atmosphere in the short-wave spectral region varies during the day under summer conditions only slightly and amounts to 0.6–0.8 km, while nearby $\lambda = 1.06$ μm it is 0.25–0.4 km, that is, the height of homogeneous aerosol atmosphere decreases with the increase of wavelength. However, under very clear conditions a weakly pronounced maximum is observed in the spectrum at $\lambda = 0.52–0.56$ μm, which is assumingly caused by particles of a medium size.

This paper undertakes, for the first time, an attempt to determine the height of the homogeneous aerosol atmosphere in a wavelength region $\lambda = 0.44–3.9$ μm.

Measurement conditions and instrumentation

To accomplish this task, we have carried out, near Tomsk since May 15 through July 7 of 2002, a series of synchronous measurements of transmittance of the entire atmospheric column and of the surface layer at the wavelengths $\lambda = 0.44$, 0.48, 0.52, 0.56, 0.69, 0.87, 1.06, 1.60, 2.20, and 3.91 μm.

The measurements in the surface layer were conducted with a filter photometer[9] on a path 830 m long with the period of 2 h (12 cycles a day). For one cycle (~ 30 min), six spectra in the wavelength region of 0.44–1.06 μm and four in the wavelength region of 1.06–3.91 μm were recorded and then averaged. The obtained values of atmospheric transmittance were used to find the spectral coefficients of total radiation extinction $\varepsilon(\lambda)$, from which then the aerosol extinction coefficients $\alpha(\lambda)$ were determined using the apparatus of multiple linear regression.

The transmittance of the entire atmospheric column was measured with a multiwave sun photometer.[10] The measurements were conducted in short series, when the sun was not screened by clouds. The data obtained were used to calculate hourly mean values of the transmittance. The molecular absorption of radiation by the gaseous constituents of the atmosphere was taken into account and the aerosol optical depth $\tau^a(\lambda)$ was separated out with the use of LOWTRAN-7 database.

For 33 days, a total of 160 simultaneously measured spectral dependences of the parameters $\tau^a(\lambda)$ and $\alpha(\lambda)$ were obtained. All optical measurements were accompanied by observations of meteorological parameters of the atmospheric surface layer, including: the temperature of the air t, the relative RH and the absolute humidity a of the air, the water vapor partial pressure e, the atmospheric pressure P, and wind velocity V. The mean values of the meteorological parameters, their standard deviations (SD), and the range of variability are summarized in Table 1. Note that the wide range of variability of these parameters is indicative of the representativeness of the data array obtained.

Table 1. Statistical characteristics of meteorological parameters of the atmosphere in the period of measurements

Parameter	Mean value	SD	max	min
t, °C	19.7	5.48	31.4	5.50
e, mbar	9.9	3.53	19.3	4.19
RH, %	43	15.8	92.0	18.0
a, g/m^3	7.3	2.56	14.2	3.25
P, Torr	743.8	4.62	753	734
V, m/s	3.4	1.65	7.90	0.0

Measurement results

The statistical processing of data of optical measurements yielded the mean values of the parameters $\alpha(\lambda)$ and $\tau^a(\lambda)$, their standard deviations, and the autocorrelation coefficients $\rho_{\alpha\alpha}$ and $\rho_{\tau\tau}$, which are presented for several wavelengths in Tables 2 and 3. It can be seen from the tabulated data that the autocorrelation matrices of the parameters $\alpha(\lambda)$ and $\tau^a(\lambda)$ differ markedly. This becomes clearer from the analysis of the autocorrelation coefficients $\rho_{\alpha(0.44)\alpha(\lambda)}$ and $\rho_{\tau(0.44)\tau^a(\lambda)}$, characterizing the relation between the variations of the parameters α and τ^a at the wavelength $\lambda = 0.44$ μm with those at other wavelengths. It can be seen that in the surface layer (Table 2) this array is characterized by a rather close correlation between the variations of the coefficients $\alpha(0.44)$ and $\alpha(\lambda)$ in the entire wavelength range (the coefficients $\rho_{\alpha(0.44)\alpha(\lambda)}$ range from 0.94 to 0.74 at the significance level ~ 0.17). This indicates that coarse aerosol contributes significantly to the variability of the parameter $\alpha(\lambda)$ through the entire spectral region studied. For the aerosol optical depth (Table 3), the autocorrelation coefficient $\rho_{\tau(0.44)\tau^a(\lambda)}$ decreases quite quickly with the increase of wavelength, and in the region $\lambda \geq 1.06$ μm it achieves the level ~ 0.50. This behavior of the coefficient $\rho_{\tau(0.44)\tau^a(\lambda)}$ shows that in the visible spectral region the coarse aerosol contributes much weaker to variations of the optical depth of the entire atmospheric column as compared to that of the surface layer.

Figure 1 depicts the spectral dependences of the parameters τ^a, α, and H_0, averaged over the period of measurements, along with their standard deviations.

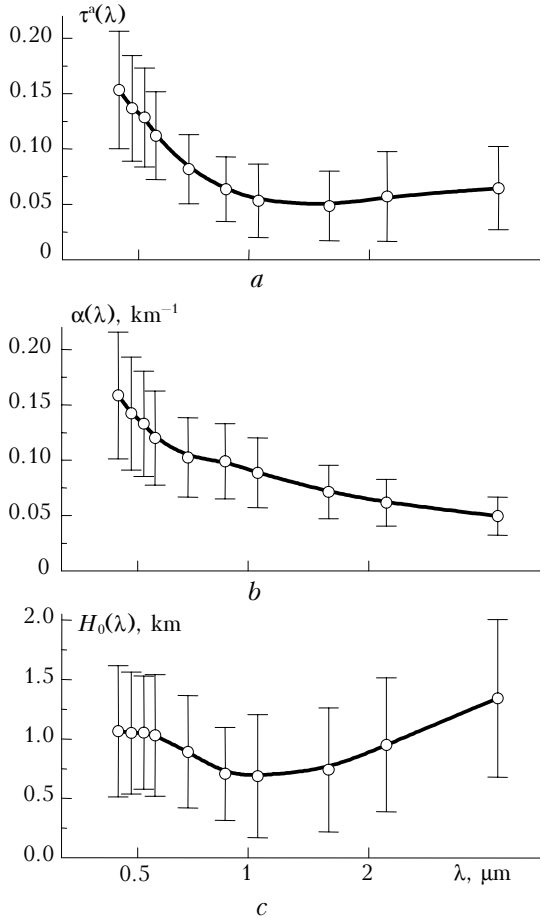

Fig. 1. Spectral dependence of the parameters $\tau^a(\lambda)$, $\alpha(\lambda)$, and $H_0(\lambda)$, averaged over the array of data obtained since May 15 through July 7 of 2002 near Tomsk.

Table 2. Statistical characteristics of the aerosol extinction coefficient $\alpha(\lambda)$

λ, μm	$\bar{\alpha}(\lambda)$, km^{-1}	SD, km^{-1}	Autocorrelation coefficients $\rho_{\alpha(\lambda)\alpha(\lambda)}$						
			α(0.44)	α(0.56)	α(0.69)	α(0.87)	α(1.06)	α(2.2)	α(3.9)
0.44	0.159	0.057	1	0.94	0.92	0.88	0.85	0.75	0.74
0.56	0.120	0.043		1	0.98	0.97	0.90	0.82	0.82
0.69	0.103	0.036			1	0.97	0.93	0.84	0.84
0.87	0.099	0.034				1	0.94	0.89	0.88
1.06	0.089	0.032					1	0.93	0.90
2.2	0.062	0.021						1	0.93
3.9	0.050	0.017							1

Table 3. Statistical characteristics of the aerosol optical depth

λ, μm	$\tau^a(\lambda)$	SD	Autocorrelation coefficients $\rho_{\tau^a(\lambda)\tau^a(\lambda)}$						
			τ^a(0.44)	τ^a(0.56)	τ^a(0.69)	τ^a(0.87)	τ^a(1.06)	τ^a(2.2)	τ^a(3.9)
0.44	0.153	0.053	1	0.97	0.83	0.72	0.50	0.45	0.52
0.56	0.112	0.040		1	0.93	0.85	0.65	0.50	0.56
0.69	0.082	0.031			1	0.94	0.81	0.50	0.52
0.87	0.064	0.029				1	0.85	0.48	0.50
1.06	0.053	0.033					1	0.39	0.36
2.2	0.057	0.041						1	0.89
3.9	0.065	0.038							1

It can be seen that for this array the averaged spectral dependence of the aerosol optical depth $\tau^a(\lambda)$ (Fig. 1*a*) decreases quickly in the wavelength region from 0.44 to 1.06 μm, then remains at the same level and even increases somewhat at the wavelength $\lambda = 3.9$ μm. At the same time, the dependence $\alpha(\lambda)$ (Fig. 1*b*) looks like a function decreasing with the wavelength in the entire spectral region.

The features discovered in the behavior of the dependences $\tau^a(\lambda)$ and $\alpha(\lambda)$ naturally manifested themselves in the averaged spectral structure of $H_0(\lambda)$ as well (Fig. 1*c*). It can be seen that in the region from 0.44 to 0.56 μm the height of the homogeneous atmosphere is about 1100 m, then it gradually decreases down to 690 m at $\lambda = 1.06$ μm. But the surprising fact is that, further into the IR region, H_0 again increases and near $\lambda = 3.9$ μm it takes the value of 1340 m.

From the general consideration, we should expect the decrease of $H_0(\lambda)$ with the increase of wavelength, because in this case the contribution of increasingly larger particles, whose concentration in the surface layer should be higher, to the aerosol extinction increases.

It is obvious that the obtained spectral dependence of the parameter H_0 is a consequence of the anomalous spectral behavior of the parameter $\tau^a(\lambda)$ in the region of λ from 1 to 3.91 μm (see Fig. 1*a*).

Quite similar spectral dependence of τ^a in the IR region can be connected, in particular, with the presence of relatively narrow fractions of particles in the atmosphere, which leads to weakly pronounced extremes of $\tau^a(\lambda)$ in the range of the main peak of the radiation extinction factor K_ρ.

The estimates show that in this case the value of $\Delta\tau^a = \tau^a(4\ \mu m) - \tau^a(1\ \mu m)$ is equal to 0.01–0.03 when passing the peak of K_ρ. For example, for non-absorbing particles with the refractive index $m = 1.5$ the relative particle size $\rho = 2\pi r/\lambda$ in the range of the main peak is 4.5. As a consequence, the fraction of particles of radius $r \sim 3$ μm forms a peak of τ^a near $\lambda = 4$ μm, and in the wavelength range from 1 to 4 μm the values of $\tau^a(\lambda)$ increase.

In addition to the averaged spectral dependences of the parameters $\tau^a(\lambda)$, $\alpha(\lambda)$, and $H_0(\lambda)$, it was interesting to analyze their dynamics at different levels of aerosol turbidity in the atmosphere. For this purpose, the primary array of empirical data was divided into four sub-arrays in accordance with the range of variability of the parameters τ^a and α at the wavelength $\lambda = 0.56$ μm.

Figure 2 shows the spectral dependences of the aerosol optical depth, the aerosol extinction coefficients, and the height of the homogeneous atmosphere for four fixed values of $\alpha(0.56)$. The same dependences for four fixed values of the parameter $\tau^a(0.56)$, are shown in Fig. 3. It can be seen from Fig. 2 that the spectral dependences $\alpha(\lambda)$ at any turbidity values decrease smoothly with the increase of wavelength (Fig. 2*b*). At the same time, the spectral dependence $\tau^a(\lambda)$ decrease continuously through the entire wavelength region only under the clearest conditions (Fig. 2*a*, curve *1*), and then, with the increase of the surface layer turbidity, the increasingly pronounced growth of $\tau^a(\lambda)$ is observed in the 1.6 to 3.9 μm region.

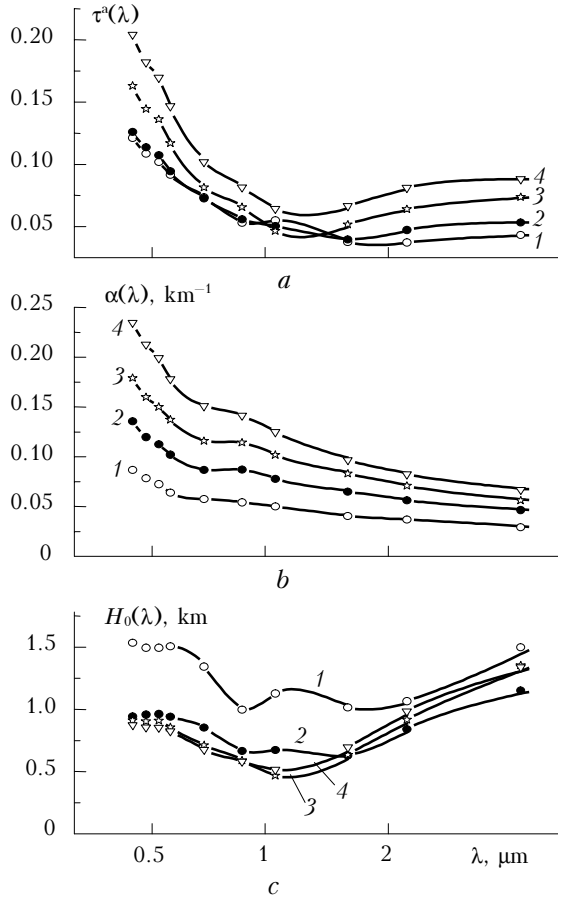

Fig. 2. Transformation of spectral dependences of the aerosol optical depth $\tau^a(\lambda)$, the aerosol extinction coefficients $\alpha(\lambda)$, and the height of the homogeneous aerosol atmosphere $H_0(\lambda)$ at $\alpha(0.56) = 0.06$ (curve *1*), 0.10 (*2*), 0.14 (*3*), and 0.18 km^{-1} (*4*).

As to the spectral dependences $H_0(\lambda)$ (Fig. 2*c*), it can be noted that the maximum height of the homogeneous aerosol atmosphere takes place under conditions of high visibility in the surface layer. As the turbidity of the surface layer increases, $H_0(\lambda)$ decreases in the entire wavelength region and, especially, in the short-wave range.

The analysis of data shown in Fig. 3 indicates that if the aerosol optical depth is used as a fixed parameter, then, naturally, $H_0(\lambda)$ is lowest at smallest values of $\tau^a(0.56)$ and highest at the largest ones. In general, the spectral dependence of $H_0(\lambda)$ shown in Fig. 2 is similar to that shown in Fig. 3.

To study the diurnal dynamics of the discussed parameters, we have separated out a sub-array that includes 14 fine days from the complete data array.

For this sub-array, Figure 4 shows the spectral dependences $\tau^a(\lambda)$, $\alpha(\lambda)$, and $H_0(\lambda)$ obtained in the morning (curves *1*), day (*2*), and evening (*3*).

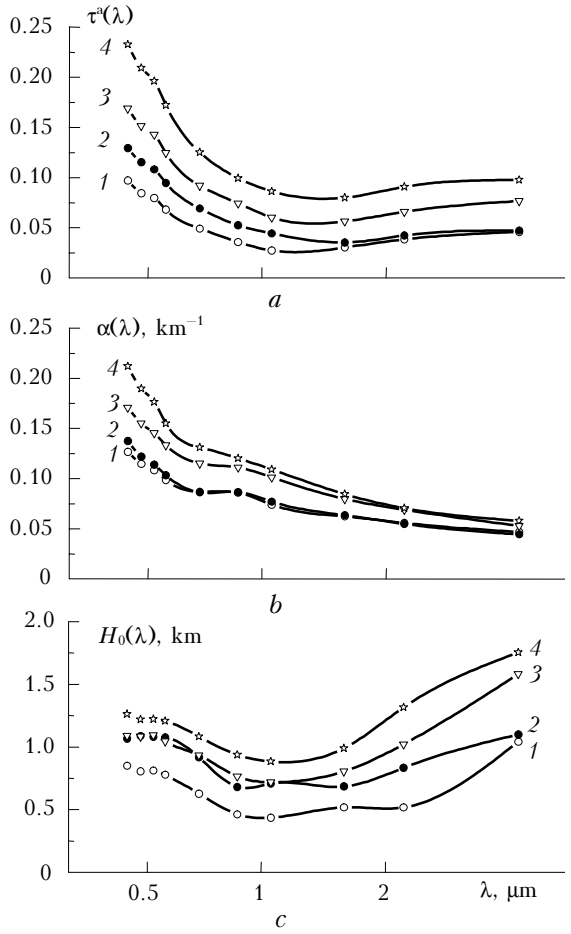

Fig. 3. Transformation of spectral dependences of the aerosol optical depth $\tau^a(\lambda)$, the aerosol extinction coefficients $\alpha(\lambda)$, and the height of homogeneous aerosol atmosphere $H_0(\lambda)$ at $\tau^a(0.56) = 0.07$ (curve *1*), 0.10 (*2*), 0.14 (*3*), and 0.17 (*4*).

As can be seen, $\alpha(\lambda)$ increase from the morning to the evening almost neutrally over the spectrum (Fig. 4*b*), which is likely connected with the convective transport of large particles from the surface aloft. In the spectral dependences of $\tau^a(\lambda)$ in the IR region, we can also see the increase of the atmospheric content of the coarse aerosol during a day (Fig. 4*a*). However, at the same time, the parameter $\tau^a(\lambda)$ in the visible spectral region varies only slightly. This circumstance, against the background of the increasing concentration of coarse particles, can be explained only by the corresponding decrease of the optical influence of fine particles in the upper atmosphere. In this case, it is difficult to say which particular mechanism affects the concentration or optical properties of fine particles. The daily transformation of the height of the homogeneous atmosphere is shown in Fig. 4*c*, from which it can be seen that in the short-wave spectral region the maximum values of H_0 are observed in the morning and then decrease somewhat. In the IR region ($\lambda = 1.6$–3.9 μm), on the contrary, the minimum values of the parameter $H_0(\lambda)$ are observed in the morning, while at the day and evening the height of homogeneous aerosol atmosphere increase markedly.

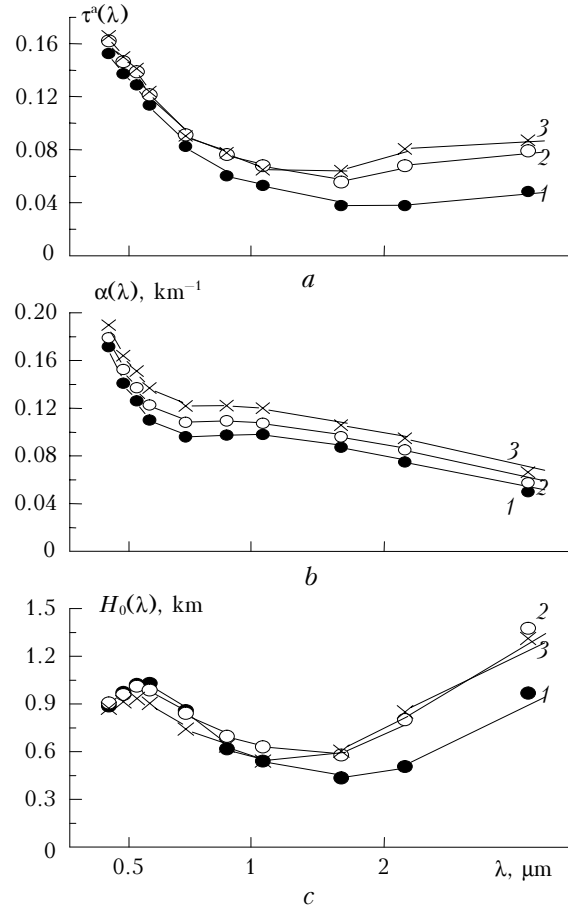

Fig. 4. Spectral dependence of the aerosol optical depth $\tau^a(\lambda)$, the aerosol extinction coefficients $\alpha(\lambda)$, and the height of the homogeneous aerosol atmosphere $H_0(\lambda)$, averaged over 14 fine days in May– June of 2002 in the morning (curves *1*), day (*2*), and evening (*3*).

Note that the minimum diurnal dynamics of $H_0(\lambda)$ is observed near the wavelength of 1.06 μm, which is most sensitive to variability of particles of the medium-size fraction.

Conclusions

1. Based on the data of simultaneous measurements of the spectral transmittance of the atmosphere along an extended surface path and in the whole atmospheric depth, we have obtained, for the first time, the field data on the height of homogeneous aerosol atmosphere in a wide wavelength range ($\lambda = 0.44$–3.9 μm) for summer period.

2. It has been found that the spectral dependence of the height of homogeneous aerosol atmosphere has a weak peak in the visible spectrum, a minimum nearby $\lambda \sim 1$ μm, and exhibits a

pronounced increase in a wavelength region of 1.6–3.9 μm.

3. The diurnal dynamics has been revealed in the spectral dependence of the height of homogeneous aerosol atmosphere. The dependence $H_0(\lambda)$ has been shown to have a maximum in the visible spectrum in the morning hours. At the wavelength near $\lambda = 3.9$ μm the maximum occurs in the daytime and in the evening.

Acknowledgments

This work was supported, in part, by the Russian Foundation for Basic Research (Grant No. 04-05-65179).

References

1. K.Ya. Kondratyev, Atmos. Oceanic Opt. **15**, No. 2, 105–124 (2002).
2. K.Ya. Kondratyev, Atmos. Oceanic Opt. **15**, No. 4, 267–284 (2002).
3. K.Ya. Kondratyev, Atmos. Oceanic Opt. **16**, No. 1, 1–12 (2003).
4. Yu. Hongbin, S.C. Liu, and R.E. Dickinson, J. Geophys. Res. D **107**, No. 12, AAC3/1–AAC3/14 (2002).
5. C. Tomasi, J. Appl. Meteorol. **21**, No. 7, 931–944 (1982).
6. V.V. Lukshin, G.I. Gorchakov, and A.S. Smirnov, in: *Results of Combined Aerosol Experiment ODAEKS-87* (TSC SB AS USSR, Tomsk, 1989), pp. 70–76.
7. S.M. Sakerin, D.M. Kabanov, Yu.A. Pkhalagov, and V.N. Uzhegov, Atmos. Oceanic Opt. **15**, No. 4, 285–291 (2002).
8. Yu.A. Pkhalagov, V.N. Uzhegov, D.M. Kabanov, and S.M. Sakerin, Atmos. Oceanic Opt. **16**, No. 8, 652–657 (2003).
9. Yu.A. Pkhalagov, V.N. Uzhegov, and N.N. Shchelkanov, Atmos. Oceanic Opt. **5**, No. 6, 423–425 (1992).
10. D.M. Kabanov, S.M. Sakerin, and S.A. Turchinovich, Atmos. Oceanic Opt. **14**, No. 12, 1067–1074 (2001).